Int. J. Electrochem. Sci., 7 **(2012)** 11281 - 11296

International Journal of
ELECTROCHEMICAL
SCIENCE
www.electrochemsci.org

Effects of Sulfate Reducing Bacteria on Corrosion of Carbon Steel Q235 in Soil-Extract Solution

Jin Xu[*], *Cheng Sun, Maocheng Yan, Fuhui Wang*

State Key Laboratory for Corrosion and Protection, Institute of Metals Research, Chinese Academy of Sciences, Shenyang 110016, China
[*]E-mail: xujin@imr.ac.cn

Received: 25 September 2012 / *Accepted:* 18 xxx 2012 / *Published:* 1 November 2012

Effects of sulfate reducing bacteria on corrosion of the carbon steel Q235 have been investigated in soil-extract solutions (SES). The results show that SRB dramatically decreases the corrosion rate of the carbon steel due to the reason that SRB increases the protective ability of the films. Elements S are observed under the corrosion products of the steel, but not on the surface of the products. SRB promotes the alkalization of the SES. The procedures of SRB influenced corrosion are described.

Keywords: SRB; EIS; Weight loss; carbon steel Q 235; soil-extract solution

1. INTRODUCTION

Microbiologically influenced corrosion (MIC) of the metals has been widely found in soil and water environments [1-9]. Sulfate-reducing bacteria (SRB) is the most important microbe for anaerobic corrosion of buried pipelines in soils [10]. SRB can remove molecular hydrogen from the cathode, leading to cathodic depolarization of the metal surface [11]. Iron sulfide by SRB is accumulated on surfaces of metals, which accelerates the dissolution of the iron [12-16].

There are plenty of studies on SRB influenced corrosion of metals. Most of them show that SRB accelerated the corrosion of metals, Torres-Sanchez et al. [17] have observed high density and low depth pitting on the surface of the stainless steel AISI 304 exposed to action of SRB. Lee et al. [12] have found that corrosion rates of mild steel are accelerated in the presence of SRB once the iron sulfide particle contacts the metal surface. Sun et al. [18-19] have concluded that SRB will accelerate the corrosion rates of zinc in soils. The experiment by Li et al. [20] have showed that the corrosion potential and polarization resistance of copper alloys drastically move towards negative direction as the SRB is in the logarithm phase.

Other researchers have recently found that sulfide films, which were metabolite of SRB, had protective effects on the metal substrate [21-26]. Most of them mainly focus on the protective effects of the sulfide on the metals in the cultured solution or the seawater. However, whether biotic sulfide has protective ability or not is seldom studied in soil environments.

In this study, the effects of SRB on the corrosion behavior of the carbon steel Q235 are investigated in the soil-extract solutions (SES) by using weight loss, electrochemical impedance spectroscopy (EIS), Scanning Electron Microscopy (SEM), Energy-dispersive X-ray analysis (EDAX) and X-ray photoelectron spectra (XPS).

2. EXPERIMENTAL

2.1. Coupon preparation

Sample of 15×15×3mm were cut from plate of carbon steel Q235 with nominal composition (wt%) of 0.30%C, 0.019%P, 0.029%S, 0.01%Si, 0.42%Mn, and balance Fe, then embedded in epoxy resin to prepare test sample with an exposed surface area of 2.25 cm^2 for electrochemical measurements. The coupons were abraded to $1000^{\#}$ with a series of grit papers followed by cleaning in acetone and alcohol and dried.

2.2. Soil solution preparation

Soils used in this study were taken from Shenyang, China. The SES was prepared by extracting the soil solution with the water-soil ratio of 5:1 (wt%). The analysis results of the solution compositions were given in Table 1. The SES was autoclaved at 121℃ for 20 min and stored at 4℃ before use.

Table 1. Compositions of the SES (mg/L)

pH	chemical composition							organic content	whole nitrogen content	total salt content
	Cl^-	SO_4^{2-}	HCO_3^-	Ca^{2+}	Mg^{2+}	K^+	Na^+			
7.38	17	139	83	15	23	6	51	25500	1050	334

2.3. Microorganisms

In order to investigate MIC of carbon steel Q235 in soil environments, SRB stains used in this study, *Desulfovibrio desulfuricans*, was isolated from soils. They were anaerobically incubated in API RP-38 medium (g/L) [27], containing $MgSO_4 \cdot 7H_2O$ 0.2; ascorbic acid 1.0, NaCl 10.0, KH_2PO_4 0.5, Sodium lactate 4.0, Yeast extract 1.0, $Fe(NH_4)_2(SO_4)_2$ 0.02, for enrichment, and was subsequently

purified in sterile agar plates using API RP-38 medium by picking up several single black colonies with a sterile inoculation loop.

20 mL of the culture containing SRB were subsequently transferred into individual 1000 ml of sterilized SES. After 2 days incubation, the abraded coupons were hung in the medium with the bacteria in a sealed jar (1000 ml) for the corrosion experiments

SRB numbers were determined by the three tube multiple most probable number (MPN) with three parallel method.

2.4. EIS analysis

EIS was used to investigate the electrochemical properties of the corroded surface after immersion in SES with SRB over time. All experiments were performed in a three-electrode electrochemical cell, with a platinum electrode used as the counter electrode, and a saturated calomel electrode (SCE) as the reference electrode. The test were operated using the PARSTAT 2273 electrochemical measurement system manufactured by EG&G. The frequency range was from 0.001 Hz to 100 kHz and the amplitude of the sinusoidal voltage signal was 10 mV. The EIS data obtained were modeled and simulated using the Zsimpwin software supplied by the PARSTAT2273.

2.5. Weight loss measurement

Rectangular coupons (40×20×3mm) were used for weight loss tests. Before tests, samples were ground down to 800 SiC-paper, degreased in acetone, sterilized by ultraviolet and weighed to a precision of 0.1mg. After corrosion test, the sample was extracted, pickled in the solutions, which contained HCl (ρ=1.19 g/ml) 500ml, hexamethylene tetramine 3.5g, distilled water 500ml, for 10 min at 25℃, cleaned with water, dried at 105℃ for 30 min in a furnace, cooled, then weighted again. The measured weight-loss was converted into uniform corrosion rate (mm/a). Triplicate samples were used for each test to guarantee the reliability of the results.

2.6. SEM, EDAX and XPS analysis

In the SEM study, the surface appearance of carbon steel Q235 in SES was visualized after preparation using the following procedure. Samples were fixed with 3% glutaraldehyde in a phosphate buffer solution (PBS, pH 7.3–7.4) for more than 4 h, and then washed with PBS for two changes (5 min each), rinsed with distilled water for another two changes (5 min each), and dehydrated with using an ethanol gradient (at 50%, 75%, 95% and 99% for 10 min) before being finally stored in a desiccator. A scanning electron microscope (XL30-FEG) with the beam voltage at 30 kV was used to visualize the morphology of surface. XPS (ESCALAB250) was used to analyze the element distributions in the corrosion products.

3. RESULTS

3.1. Variation of SRB numbers

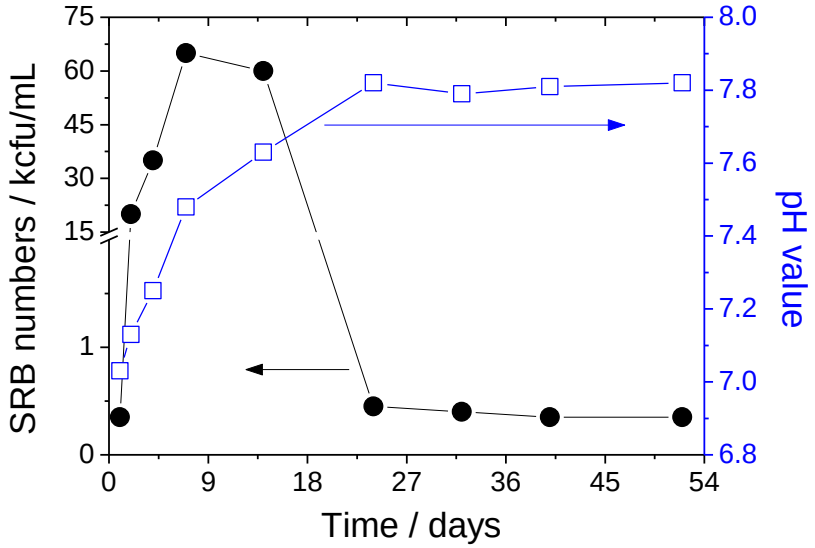

Figure 1. SRB numbers and pH values with time in SES with SRB

Fig. 1 shows the SRB numbers and pH values with time in the SES with SRB. As shown in Fig. 1, the SRB numbers rapidly increase with time from 350 at the first day to 65000 cfu/mL after 7 days, slowly decrease to 60000 cfu/mL after 14 days, dramatically decrease to 450 cfu/mL after 24 days, and then remain stable. The pH value increases with time, reaches a peak after 24 days, and then remains stable.

The following reactions occur in the presence of SRB [23]:

$$4Fe + SO_4^{2-} + 4H_2O \rightarrow FeS + 3Fe(OH)_2 + 2OH^-$$

The above equation indicates that the pH value will increase after adding SRB. The pH value sharply increases with SRB numbers increasing from 1 day to 7 days during the growth period, slowly increases with dying of SRB from 7 days to 24 days because there are still large numbers of SRB in the SES, and then remains stable after 24 days because there are few SRB in the SES.

The above results show that SRB promotes the alkalization of the SES.

3.2. SEM and EDAX analysis

Fig. 2 shows the micrograph appearance of the carbon steel Q235 in the SES with and without SRB after 52 days. There is a dense film appearing micro-crack structure on the surface of the corrosion products of the carbon steel in the SES with SRB. The products with blowball structure adhere on the surface of the film. The intact film is not observed on the surface of the carbon steel, and

the surface is also adhered by a few blowball products. As shown in Table 2, there are few elements S on the surface of the corrosion products of the carbon steel in the presence of SRB.

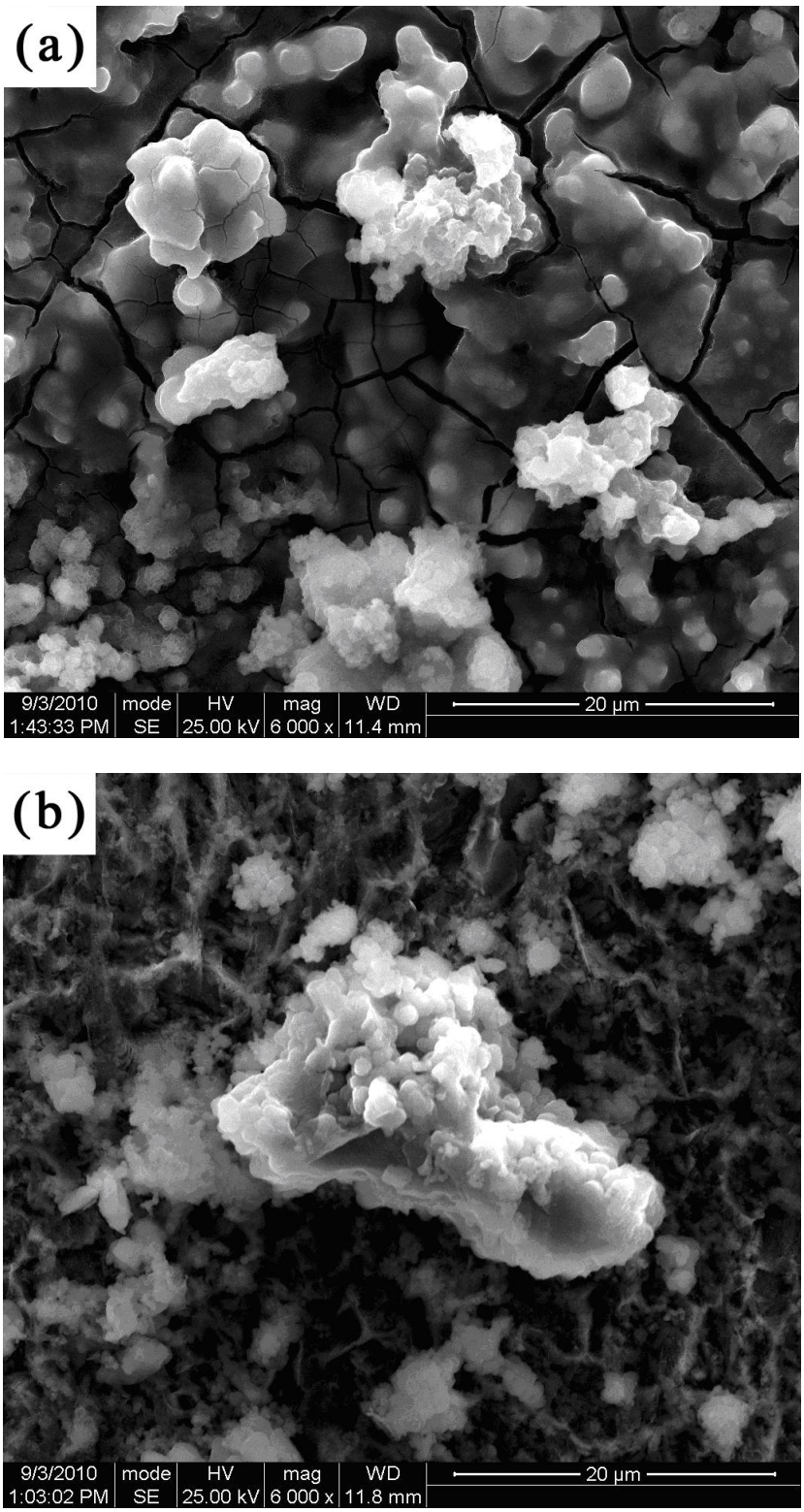

Figure 2. SEM images of the corrosion products in the SES with and without SRB (a-with SRB; b-without SRB)

Elements C are observed for the products with SRB, which is due to the existence of high-molecular compounds in the biofilms.

Table 2. EDAX results of the corrosion products of carbon steel Q235 (atom%)

Element	O	Fe	C	S	Si	Cl	K
With SRB	61.7	22.8	11.6	-	1.73	1.12	1.01
Without SRB	69.2	23.4	-	-	4.97	0.79	1.82

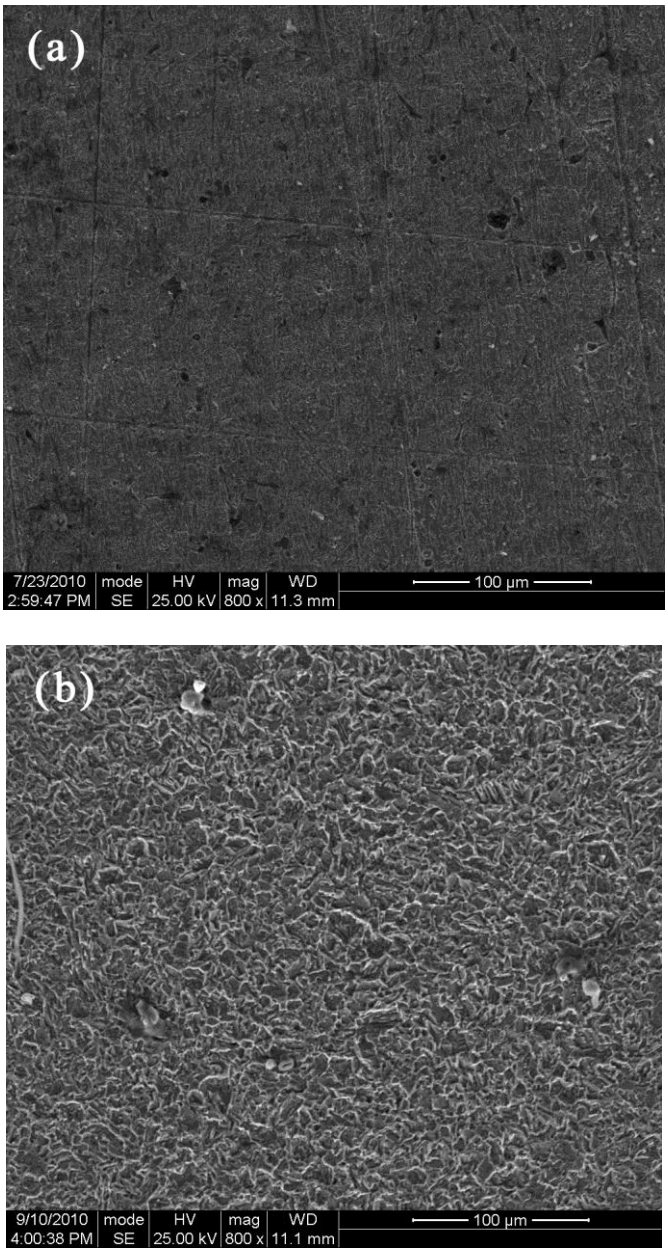

Figure 3. SEM images of the steel in the SES with and without SRB after removing the corrosion products (a-with SRB; b-without SRB)

Fig. 3 shows the appearance of the steel in the SES with and without SRB after removing the corrosion products. Amounts of Pitting holes are observed on the surface of the steel in the SES with SRB, but not in the absence of SRB. It shows that the susceptivity of the steel to corrosion was more in the SES with SRB than that without SRB, and the pitting corrosion readily occurred on the surface the steel in the presence of SRB The surface of the steel still contained the polishing grooves in the SES with SRB. However, the grooves had disappeared in the SES without SRB, which indicates that the severe corrosion has occurred.

3.3. XPS analysis

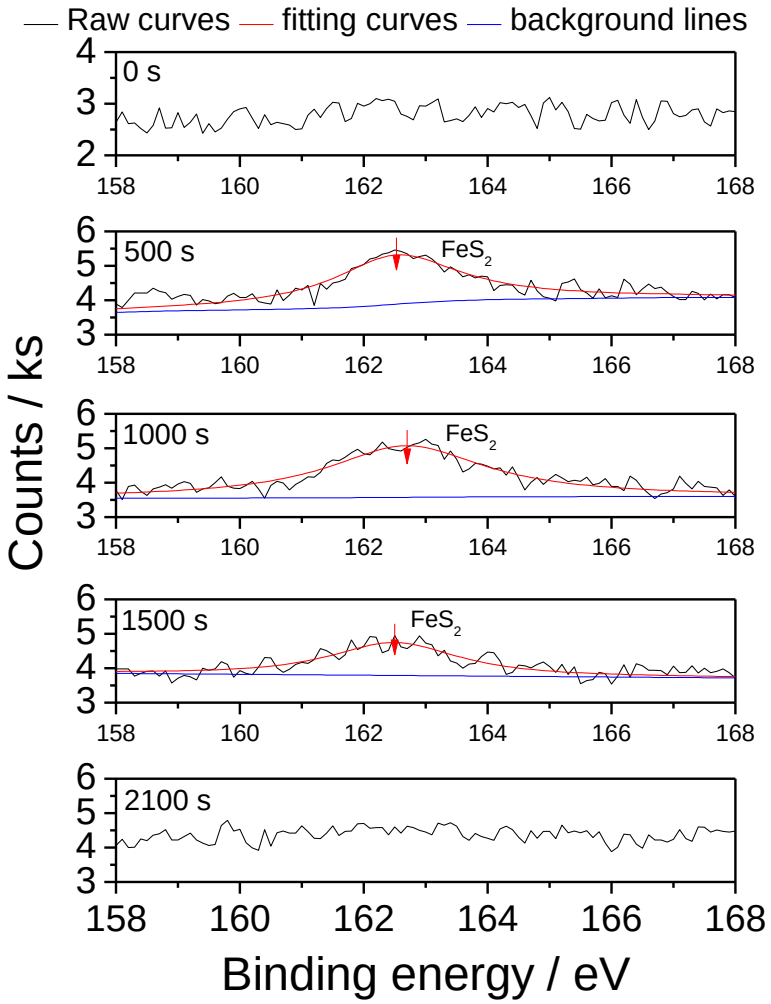

Figure 4. XPS depth profile spectra of sulfur element on the surface of the steel in the presence of SRB

XPS depth profile spectra, as shown in Fig. 4, is used to analyze the distributions of elements S in order to deeply know the sulfur changing in corrosion products of the steel in the presence of SRB. The results show that few amounts of sulfide are observed on the surface of the products, and there are elements S in the products after etching for 500 seconds. The amounts of elements S increase with the

decreasing of the distance away from the metal matrix, reaching a peak after 1000 seconds, and then decrease. The above results show that iron sulfide is formed under the corrosion products, not on the surface of the products. Sulfides formed in the bulk solution are not absorbed on the surface of the corrosion products

3.4. EIS analysis

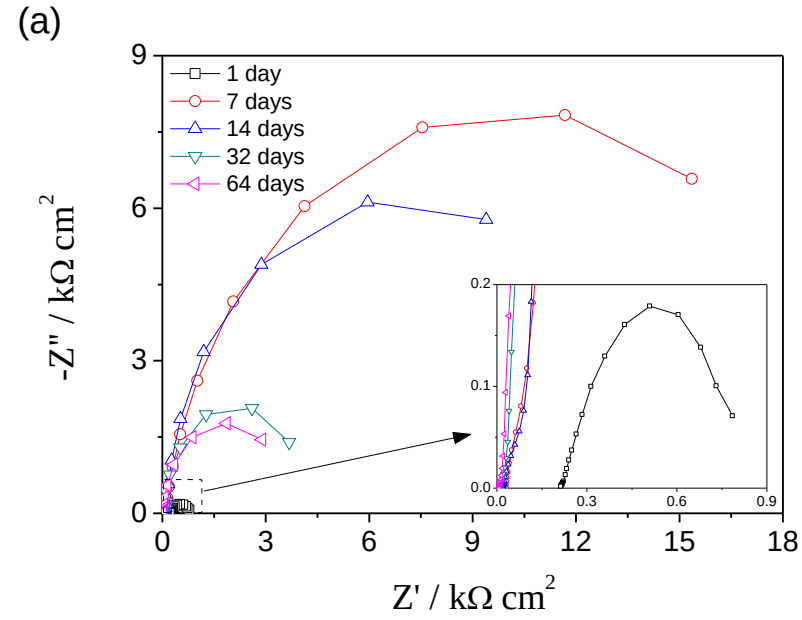

(a) Nyquist plot

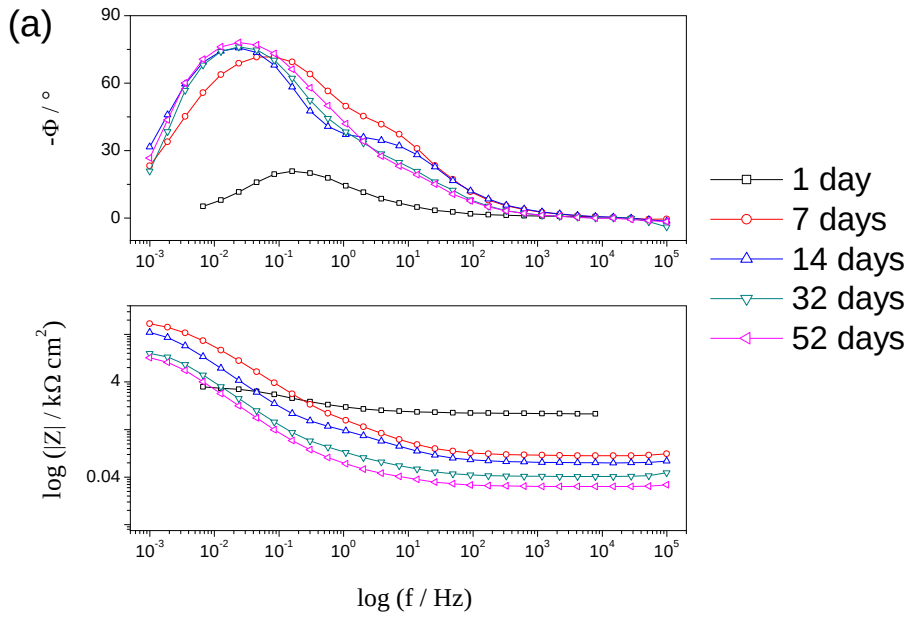

(b) Bode plot

Figure 5. EIS plots in the SES with SRB

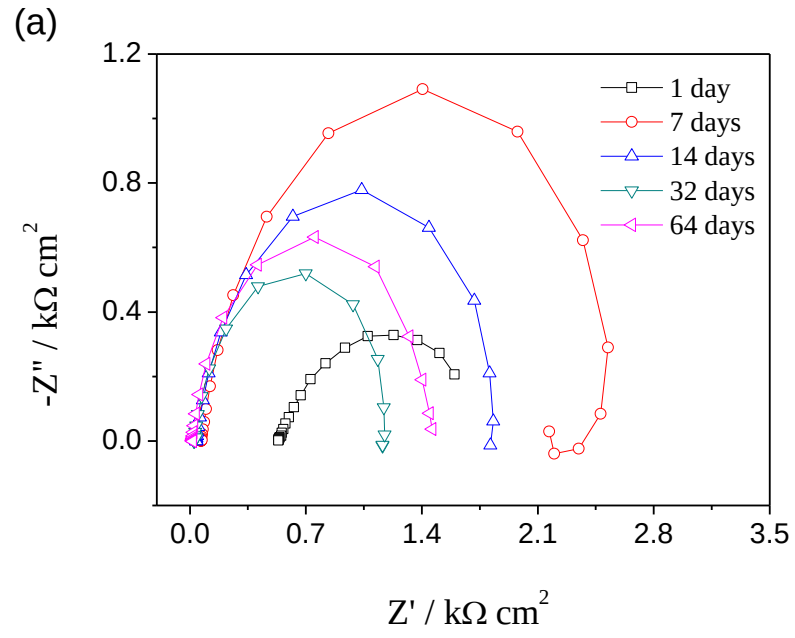

(a) Nyquist plot

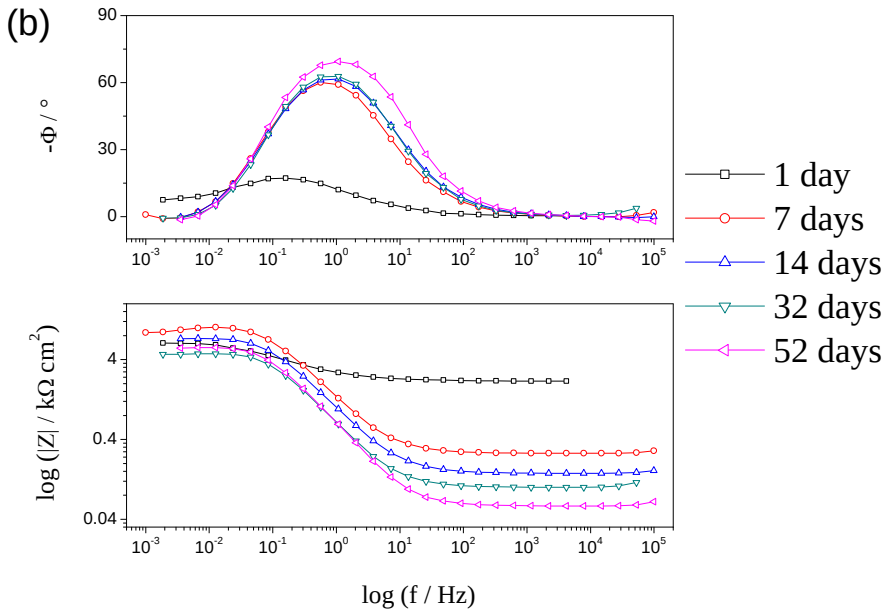

(b) Bode plot

Figure 6. EIS plots in the SES without SRB

Fig. 5 and 6 show EIS plots of the carbon steel Q235 with time in the SES with and without SRB, the corresponding equivalent circuits are given in Fig. 7, and the fitting results are listed in Table 3 and 4. In the electrical analog circuits, R_s represents an electrolyte resistance. R_f and Q_f represent a resistance and a capacitance of the corrosion product, respectively. R_{bio} and Q_{bio} represent a resistance and a capacitance of the biofilm, respectively. R_t and Q_{dl} represent a charge transfer resistance and a

double layer capacitance, respectively. R_L and L represent a resistance and an inductive during the initiation period of pitting, respectively.

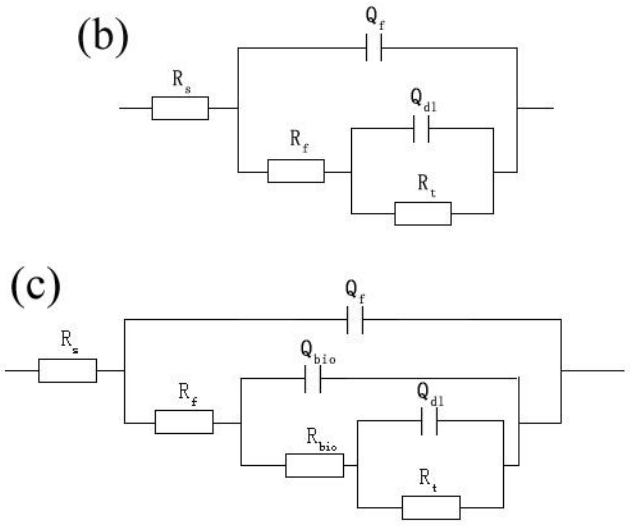

Figure 7. The equivalent circuit of EIS plots (a-Three time constants with inductive loop; b-Two time constants; c-three time constant)

Table 3. Fitting results of EIS curves in the SES with SRB

Time day	R_s Ω cm^2	R_f Ω cm^2	Y_f mS sec^n/cm^2	n_f	R_{bio} Ω cm^2	Y_{bio} mS sec^n/cm^2	n_{bio}	R_t kΩ cm^2	Y_{dl} mS sec^n/cm^2	n_t
1	214.7	111	5.609	0.6837				0.496	7.101	0.7417
7	28.07	22.37	0.6315	0.8105	275.2	0.483	0.7921	20.1	0.7053	0.9855
14	20.19	68.08	1.185	0.7992	112.1	1.246	0.9856	14.2	3.088	0.9886
32	10.66	34.69	3.788	0.8491				4.746	8.82	0.9668
52	6.494	14.34	5.281	0.881				4.08	12.22	0.9416

Table 4. Fitting results of EIS curves in the SES without SRB

Time day	R_s Ω cm^2	R_s Ω cm^2	Y_f mS sec^n/cm^2	n_f	R_t kΩ cm^2	Y_{dl} mS sec^n/cm^2	n_t	R_L kΩ cm^2	L MH cm^2
1	532.3	84.26	3.705	0.5934	1.22	0.9939	0.616	-	-
7	66.79	98.78	0.4896	0.8574	2.586	0.164	0.839	10.45	0.3113
14	37.58	67.74	1.958	0.8576	1.88	0.5969	0.843	13.12	1.313
32	25.1	46.86	1.724	0.8777	1.236	0.5152	0.8502	8.074	0.2578
52	14.65	18.57	2.837	0.9052	1.443	0.8601	0.8884		

The spectra obtained in the SES with SRB have two time constants after 1 day, three time constants after 7 days, and then two time constants after 32 days, as shown in Fig. 5 (b). The time constants at the high frequency may be due to the forming of the corrosion products and the biofilm by SRB, and the time constant at the low frequency appears because the protective ability of the films is not perfect. The radii of the capacitive loop at the low frequency increases (reaching a peak after 7 days) with time, decreases after 7 days, and then remains stable after 32 days.

Inductive loop is observed at the lowest frequency in the SES without SRB after 8 days, which is due to the presence of active pits (in Fig. 6 (b)). It is the typical features of the pitting model during the initiation period [28, 29]. The radii of the capacitive loop increase with time, decreases after 7 days, and then remains stable after 32 days.

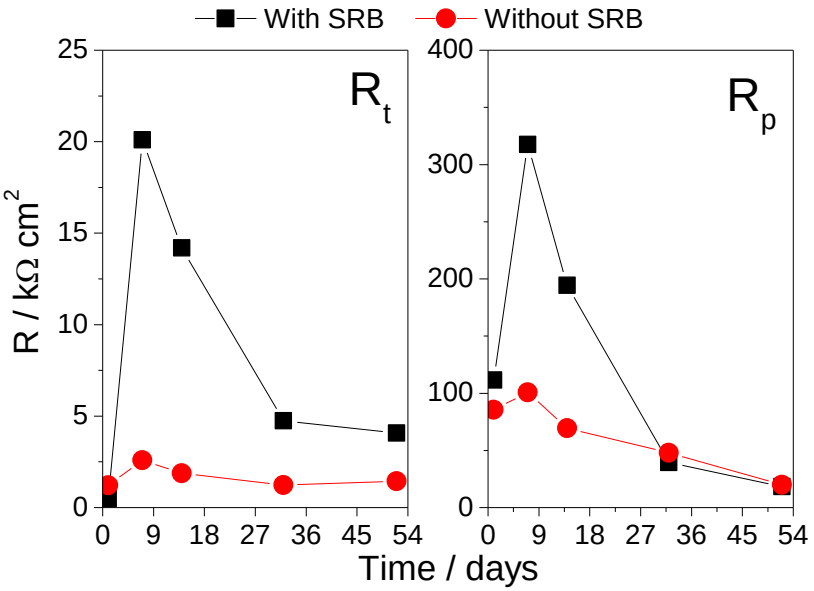

Figure 8. R_p and R_t plots in the SES with SRB and without SRB

The corrosion of the steel and the film formed on the surface is discussed in the SES with and without SRB by using the charge transfer resistance (R_t) and The polarization resistance (R_p) [29].

R_t is expressed as following relation:

$$\frac{1}{R_t} = \left(\frac{\partial I_F}{\partial E} \right)_{X_i}$$

where R_t is the charge transfer resistance, I_F is the faraday current, E is the potential, and X_i is the state variable.

R_p is expressed as following relation:

$$R_p = (Z_F)_{\omega=0} = \left(\frac{1}{Y_F}\right)_{\omega=0}$$

where R_p is the polarization resistance, ω is the frequency, and Z_F and Y_F are the faraday impedance and admittance, respectively.

The meaning of the equation shows that R_p is equal to Z_F or $1/Y_F$ when ω approaches to zero.

The results of R_p and R_t are listed in Fig. 8.

The R_t and R_p values dramatically increase with time in the presence of SRB, decrease after 7 days, and then remain stable, which is accordance with the tendency of SRB growth. The above result shows that SRB seriously influences the interface reaction of the steel and the morphology of the corrosion products. The R_t and R_p values remain stable in the absence of SRB, which indicates that there are few extraneous factors affecting the interface reaction.

The R_t and R_p values are much bigger in the SES with SRB before 32 days than those without SRB, which indicates that the biofilm, as shown in Fig. 2, is more protective than that of the corrosion product film during these periods. The above result is due to the reasons that biofioms are dense and negatively charged, which have a repulson to corrosion anion, e.g., Cl ions [28, 30, 31]. Some reports [22, 23] also show that the biofilm has a significant influence on the corrosion effect. The protective ability of the biofilm stems from the accumulation of FeS and $Fe(OH)_2$ inside the biofilm pores.

The R_p values are almost the same in the SES with and without SRB after 32 days. It indicates that the activity and electronegativity of the biofilms gradually disappear with the dying of SRB leading to decreasing of the protective ability of the films. However, the R_t value is bigger in the SES with SRB than that without SRB due to the compactability of the composite film containing the biofilm and the corrosion product film.

The above results show that SRB has a important influence on the protective ability of the films.

3.5. Weight loss analysis

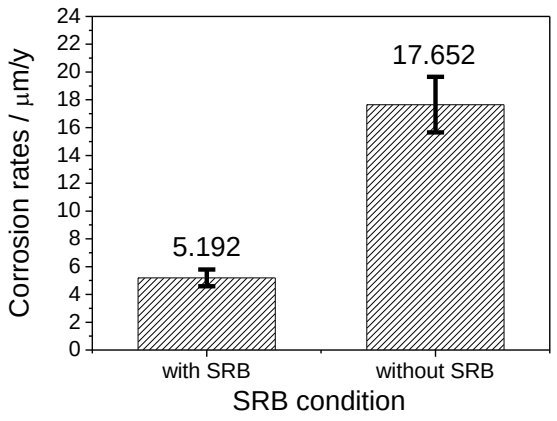

Figure 9. Corrosion rate of carbon steel Q235 in the SES with and without SRB

Fig. 9 shows the corrosion rate of the carbon steel Q235 converted by weight loss after immersing for 52 days in the SES with and without SRB. The corrosion rate of the carbon steel Q235 is much bigger in the SES without SRB than that with SRB. The rate is 17.65 μm/y in the SES without SRB and 5.19 μm /y in that with SRB. The above result shows that the average corrosion rate of the steel is lower in the SES with SRB than that without SRB.

The above result further shows that the bioflim has a good protective ability.

3.6. Procedure of SRB influenced corrosion

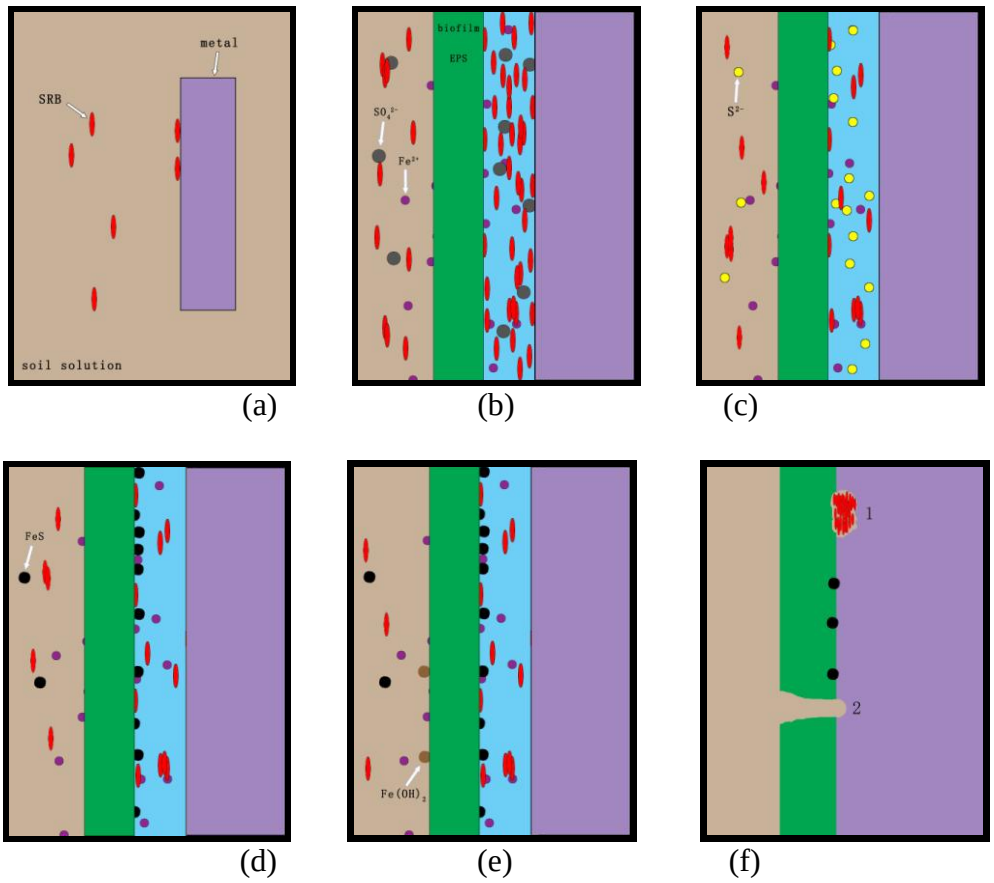

Figure 10. Diagrammatic sketch of SRB influenced corrosion

Fig. 10 shows the schematic diagram of interaction between SRB and the carbon steels, which is an idealistic and simple diagram.

The EDXA results show that S is not observed in the corrosion products on the surface of the steel, but S is found in the detached corrosion products. The results of the XPS further demonstrate that some of S elements in the detached corrosion products existe as form of sulfide. The above results show that sulphide is not absorbed on the outer surface, and may be absorbed on the inner surface or deposit on the bottom of the container by gravity. Five Figures, from Fig. 10(a) to Fig. 10(e), straightforwardly explain the reason why this phenomenon may happen.

First, a few SRB aggregate on the surface of the carbon steel Q235 when the coupon is immersed at the beginning (Fig. 10 (a)). The amounts of the sessile SRB become more and more with increasing of the planktonic SRB in the SES.

Second, with increasing of the metabolites which is due to the growing and metabolizing of the SRB, a layer of biofilm is formed on the surface of the carbon steel (Fig. 10 (b)). Here, the biofilm is described as a separate layer, the reason of which is mainly used to explain the local changing between the biofilm and the metals. The sessile SRB become more and more under the biofilm because an anaerobic environment is formed.

Third, the anions, such as sulphate ions, are pushed away from the surface of the biofilm under the effects of repulsion because of the biofilm with negative charge [25]. SRB utilize sulphate ions as the terminal electron acceptor and organic substances as carbon sources. Sulphate ions are reduced to sulphide ions during the metabolite process (Fig. 10 (c)).

Fourth, the sulphide ions react with dissolved ferrous ions to form iron sulphide, FeS, (Fig. 10 (d)). FeS inside the biofilm is absorbed on the inner surface of the biofilm.

Fifth, FeS outside the biofilm deposits on the bottom of the container by gravity (Fig. 10 (e)) which lead to no observation of S in the corrosion products on the surface of the metals. The excessive ferrous ions react with hydroxide ions to form ferrous hydroxide. Small amounts of FeS and $Fe(OH)_2$ are absorbed on the microholes of the biofilm, which increase the density of the biofilm [22, 23].

Local corrosion, especially pitting, is often observed for the MIC during the process of immersing. Fig. 10 (f) shows two typical pits. One is the pitting caused by SRB. SRB aggregate on the local surface of the carbon steel. In the course of the metabolism of SRB, hydrogen sulphide is formed. Because hydrogen sulphide is corrosive for the metal, the metals below SRB are dissolved, and eventually, pitting is formed. The other is the pitting caused by the corrosion microcell with a big cathode and a small anode. With the decreasing of the activity and the adhesion of the films, the films partially exfoliate during the death phase of SRB. The free metal acts as the anode and the films as the cathode, which leads to the forming of the microcell. Finally, the pitting is formed in the anodic region.

The following reactions occurred [23]:

$Fe \rightarrow Fe^{2+} + 2e^-$ (anodic reaction)

$H_2O \rightarrow H^+ + OH^-$ (water dissociation)

$H^+ + e^- \rightarrow H_{ads}$ (cathodic reaction)

$SO_4^{2-} + 8H_{ads} \rightarrow S^{2-} + 4H_2O$ (bacterial consumption)

$Fe^{2+} + S^{2-} \rightarrow FeS$ (corrosion products)

$Fe^{2+} + 2OH^- \rightarrow Fe(OH)_2$ (corrosion products)

$4Fe + SO_4^{2-} + 4H_2O \rightarrow FeS + 3Fe(OH)_2 + OH^-$ (overall reaction)

5. CONCLUSIONS

(1) A layer of dense biofilm is formed on the surface of the carbon steel Q235 in the SES with SRB, but not without SRB.

(2) Elements S are observed in the inner of the corrosion products of the steel, but not on the surface of the products.

(3) The results of EIS and weight loss have showed that SRB inhibits the corrosion of the steel.

ACKNOWLEDGMENTS
The project was financially supported by the National Natural Science Foundation of China (Grant No. 51131001 and 50971128), the National R&D Infrastructure and Facility Development Program of China (Grant No. 2060503).

References

1. S.Y. Li, Y.G. Kim, K.S. Jeon and Y.T. Kho, *Met. Mater*. 6 (2000) 281.
2. J. Liu, B.L. Hou, J.Y. Zheng and L.M. Xu, *Mater. Prot*. 34 (2001) 8.
3. G. Chen and C.R. Clayton, *J. Electrochiem. Soc*. 145 (1998) 1914.
4. P. Angell and J.S. Luo, *Corros. Sci*. 37 (1995) 1085.
5. B.J. Webster and R.C. Newman, *Corros. Sci*. 35 (1993) 675.
6. S.R. Torres and V.J. Garcia, *Mater. Corros*. 52 (2001) 614.
7. D.E. Nivens, P.D. Nichols and J.M. Henson, *Corrosion*, 42 (1986) 204.
8. P.J.B. Scott and M. Davies, *Mater. Performance*, 28 (1989) 57.
9. S.W. Borenstein, *Mater. Performance*. 30 (1991) 52.
10. J. Liu, J.S. Zheng and L.M. Xu, *Mater. Corros*. 52 (2001) 833.
11. G.G. Geesey, What is biocorrosion? International workshop on industrial biofouling and biocorrosion, Stuttgart, Germany. Springer, Berlin Heidelberg New York (1990).
12. W. Lee and W.G. Charachlis, *Corrosion*. 49 (1993) 186.
13. E. Schaschl, *Mater. Perform*. 7 (1980) 9.
14. R.C. Newman, W.P. Wong and A. Garner, *Corrosion*. 42 (1986) 489.
15. A. Pourbaix, L.E. Aguiar and A.M. Clarinval, *Corros. Sci*. 35 (1993) 693.
16. P.J. Antony, R.K. Singh Raman, R. Mohanram, P. Kumar and R. Raman, *Corros. Sci*. 50 (2008) 1858.
17. R. Torres-Sanchez, J. Garcia-Vargas, A. Alfonso-Alonso and L. Martinez-Gomez, *Mater. Corros.* 52 (2001) 614.
18. C. Sun and E.H. Han, *Chin. J. Nonferr. Metal*. 12 (2002) 1109.
19. C. Sun, J. Xu, F.H. Wang and C.K. Yu, *Mater. Corros.* 61 (2010) 762.
20. J. Li, Z.Y. Xu, Y.L. Du, W.T. Mou and W.G. Sun, *J. Chin. Soc. Corros. Prot.* 27 (2007) 342.
21. C.O. Obuekwe, D.W.S. Westlake, J.A. Plambeck and F.D. Cook, *Corrosion* 37 (1981) 461.
22. J.E.G. González, F.J.H. Santana and J.C. Mirza-rosca, *Corros. Sci*. 40 (1998) 2141.
23. X.X. Sheng, Y.P. Ting, and S.O. Pehkonen, *Corros. Sci.* 49 (2007) 2159.
24. B.C. Syrett, D.D. Macdonald and S.S. Wing, *Corrosion.* 35 (1979) 409.
25. B.C. Syrett and S.S. Wing, *Corrosion.* 36 (1980) 73.
26. B.C. Syrett, *Corres. Sci*. 21 (1981) 187.
27. J. Liu , L.M. Xu and J.S. Zheng, *J. Chin. Soc. Corros. Prot.* 21 (2001) 345.
28. R.J. Zuo, E. Kus, F. Mansfeld and T.K. Wood, *Corros. Sci*. 47 (2005) 279.

29. C.N. Cao, Principles of electrochemistry of corrosion (third edition), chemical industry press, Beijing, China, (2008).
30. W.A. Hamilton, S.Maxwell, Proceedings of the international conference on biologically induced corrosion (TX: NACE), Houston, (1985).
31. W.M. Dunne, *Clin. Microbiol. Rev*. 15 (2002) 155.